Hot workability evaluation of Zr-stabilized aluminium alloy 2014 by means of torsion test

J. Bidulská[1], R. Bidulský[2]*, L. Ceniga[2], T. Kvačkaj[1], M. Cabibbo[3], E. Evangelista[3]

[1]*Department of Metal Forming, Faculty of Metallurgy, Technical University Košice, Vysokoškolská 4, 042 00 Košice, Slovak Republic*
[2]*Institute of Materials Research, SAS Košice, Watsonova 47, 040 01 Košice, Slovak Republic*
[3]*INFM, University of Ancona, Via Brecce Bianche, I-60131, Ancona, Italy*

Abstract

Resulting from torsion tests, the paper deals with hot workability of the Zr-stabilized aluminium alloy 2014 to improve mechanical properties due to the presence of the Al_3Zr precipitations. In general, the torsion tests, registering values of the torque M_k along with a number of revolutions N, and consequently leading to a stress-strain curve, enable to obtain information on ductility of the investigated material. Measured at the different temperature and stress rate, T and $\dot{\varepsilon}$, respectively, the stress-strain curves exhibit rapid increase up to the peak value σ_p to be followed by a gradual decrease to the material fracture, accordingly without a steady state usually observed before the fracture. Finally, resulting from the stress decrease, and consequently using an analytical model, the relative softening RS and consequently the material fracture are determined. The presented experimental results exhibit a decrease of ductility, as a property related to workability, with an increase and a decrease of $\dot{\varepsilon}$ and T, respectively, and consequently optimal values of $\dot{\varepsilon}$, T are obtained.

K e y w o r d s: aluminium alloy, torsion test, ductility

1. Introduction

In general, aluminium alloys represent widely used materials in aircraft, aerospace, automotive and aeronautical industries due to low density and high strength, the latter improved by an addition of zirconium to result in the presence of the Al_3Zr particles [1–13]. Additionally, as presented in [10, 11], zirconium inhibits a recrystallization process of the aluminium alloys. Representing one of experimental methods, the torsion test performed at the different temperature T and the strain rate $\dot{\varepsilon}$ is usually used to obtain information on ductility to be connected, in general, with shear loading [2]. With regard to experimental conditions in laboratories, the torsion test to be used for an evaluation of workability including ductility as a material property is performed in the temperature and strain rate ranges, $T = 473$–773 K and $\dot{\varepsilon} = 10^{-3}$–$10$ s^{-1} [3–9], respectively. With regard to an analytical-experimental model presented in [14, 15], the $(\sigma - \varepsilon)$ dependence along with the strain ε and the strain rate $\dot{\varepsilon}$ is derived as

$$\sigma = \frac{\sqrt{3}M_k}{2\pi r^3}\left(3 + m + n\right), \tag{1}$$

$$\varepsilon = \frac{2\pi r N}{\sqrt{3}L}, \quad \dot{\varepsilon} = \frac{2\pi r}{\sqrt{3}L}\frac{\partial N}{\partial t}, \tag{2}$$

and the coefficients m, n have the form

$$m = \left.\frac{\partial\left(\ln M_k\right)}{\partial\left(\ln \dot{\varepsilon}\right)}\right|_{\varepsilon,T}, \quad n = \left.\frac{\partial\left(\ln M_k\right)}{\partial\left(\ln \varepsilon\right)}\right|_{\dot{\varepsilon},T}, \tag{3}$$

where M_k (N mm) is a torque; N is a number of revolutions to material fracture at the temperature T within

*Corresponding author: tel.: +421/55/792 22 51; fax: +421/55/792 24 08; e-mail address: rbidulsky@imr.saske.sk , rbidulsky@yahoo.com
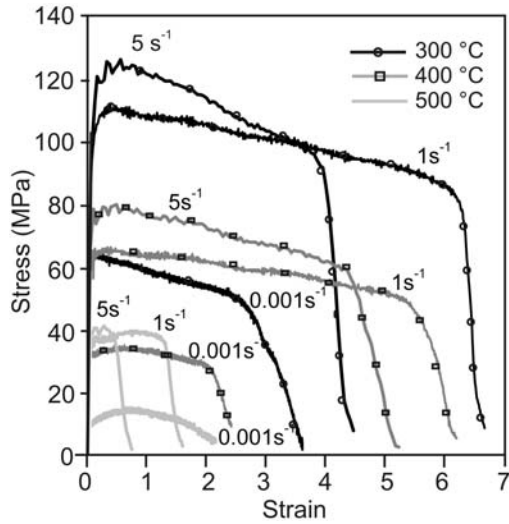
Fig. 1. Stress-strain curves of Zr-stabilized aluminium alloy 2014.

the time period t; r and L are radius and length of a sample, respectively.

2. Material and experimental procedure

The Zr-stabilized aluminium alloy 2014 investigated in this paper had the following chemical composition: Cu – 4.32 %, Mn – 0.77 %, Si – 0.68 %, Mg – 0.49 %, Fe – 0.29 %, Zr – 0.13 %, Ti – 0.03 % and Al – balance. Samples with diameter of 10 mm and length of 20 mm were machined from extruded rods. The torsion test was performed on a torsion machine at the temperature $T = 300, 350, 400, 450, 500$ °C measured by a K-type thermocouple. After an induction heating in air with a heating rate of 1 °C/s and a time holding of 3 min, the samples fixed in an axial direction were deformed to the fracture at equivalent strain rates of $10^{-3}, 10^{-2}, 10^{-1}, 1, 5$ s^{-1}, and water-quenched immediately after the deformation. Final deformation related to a number of twists to the fracture during the continuous test provides information on formability.

3. Experimental results and discussion

3.1. Stress-strain curves

As a result of the torsion test, the stress-strain curves are shown in Fig. 1 to exhibit a rapid increase to the peak stress σ_p followed by a gradual decrease towards a steady state not to be reached before the fracture, and a similar behaviour is presented in [16–20]. Considering the stress-strain curves, the temperature 300 °C is optimal with regard to formability as confirmed in [1, 15] to present similar results at 300–350 °C.
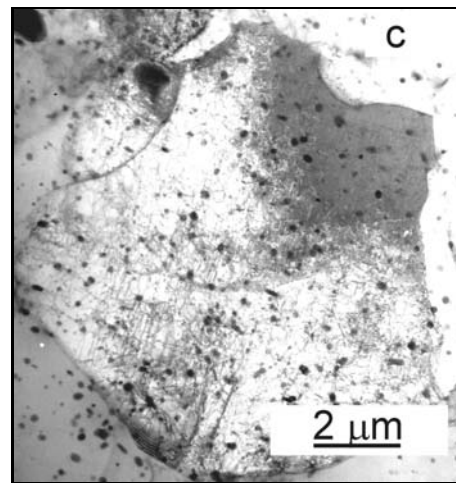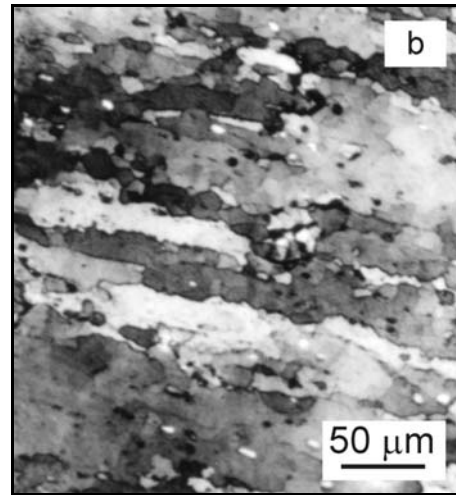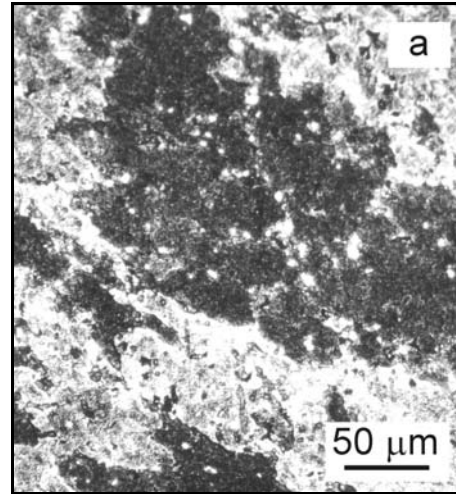

Fig. 2. (a) Microstructure of as-received sample, (b) microstructure of torsion-loaded sample for the temperature $T = 500$ °C and the deformation rate $\dot{\varepsilon} = 10^{-3}$ s^{-1} (light microscopy), (c) microstructure of torsion-loaded sample for the temperature $T = 500$ °C and the strain rate $\dot{\varepsilon} = 10^{-3}$ s^{-1} (transmission electron microscopy).

T a b l e 1. The average equivalent diameter d and the number N_V of particles per volume unit for torsion-loaded samples

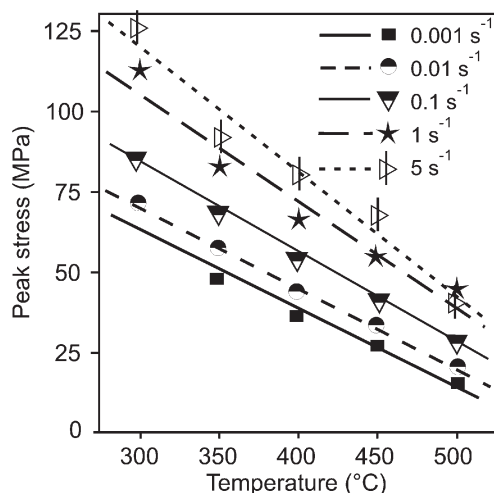| Temperature (°C)	Strain rate (s^{-1})	Diameter (nm)	Number per volume unit (10^{18} m^{-3})
300	0.001	71	14.6
300	0.1	58	14.8
400	0.001	67	15.3
400	0.1	77	17
500	0.001	78	14.6
500	0.1	65	22.3

Fig. 3. Relationship between the peak stress σ_p and the temperature T for the deformation rate $\dot{\varepsilon}$ as a parameter.

Fig. 4. Relationship between the peak stress σ_p and the deformation rate $\dot{\varepsilon}$ for the temperature T as a parameter.

3.2. Microstructures

Figure 2 shows microstructures of the as-received and torsion-loaded samples, using light and transmission electron microscopy (LM, TEM). The typical microstructure of the torsion-loaded sample consists of chains of equiaxed or slightly elongated subgrains developed inside the elongated grains (Fig. 2b). The TEM inspection revealed the presence of precipitates within the grains and subgrains observed even at higher temperature (Fig. 2c) corresponding to solution-treatment temperature [21]. Table 1 presents the average equivalent diameter d of the hardening particles and their number N_V per a volume unit, where an increase of N_V corresponding to temperature and strain rate increases results from a dissolution effect of the finest particles.

3.3. Peak stress and relative softening

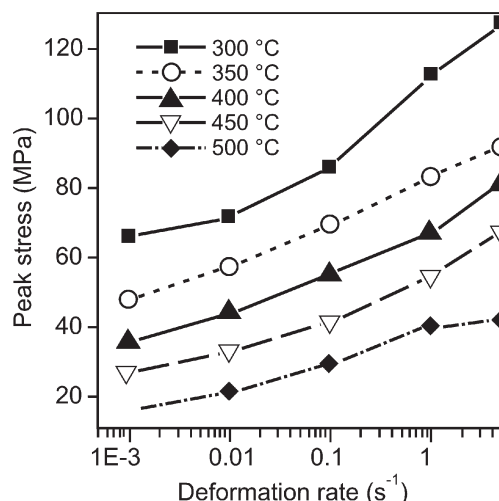Figures 3 and 4 determined from the stress-strain curves show decreasing and increasing dependences of

σ_p on temperature and the stress rate, respectively, exhibiting a maximum at 130 MPa. Additionally, the relative softening RS after σ_p, derived as [14, 19]

$$RS = \frac{\sigma_p - \sigma_{p+0.25}}{\sigma_p}, \qquad (4)$$

and shown in Fig. 5 at different temperature and deformation rate, represents an increasing function of T, except for $\dot{\varepsilon} = 5\,s^{-1}$, where $\sigma_{p+0.25}$ is a stress at $\varepsilon = 0.25$ after σ_p. The relative softening is a consequence of dynamic recovery resulting from a high dislocation density leading to formation of subgrains. With regard to [19], finer particles to be responsible for higher strength are also able to intensively coalesce to result in intensive softening.

The paper [20] presents an investigation of the aluminium alloy 6015 to exhibit higher value of σ_p and RS at $T = 300\,°C$ and $\dot{\varepsilon} = 0.1\,s^{-1}$ to be associated with higher density of very fine particles to support growth of subgrain density. According to [22], higher concentration of Mg_2Si is caused by σ_p and RS.
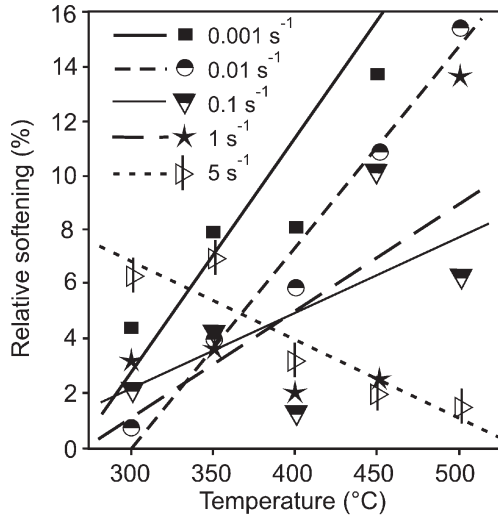
Fig. 5. Relationship between the relative softening RS, the temperature T and the strain rate $\dot{\varepsilon}$.

3.4. Fracture strain

In general, the fracture strain ε_f is considered to represent ductility of a material. The relationship $\varepsilon_f = \varepsilon_f(T, \dot{\varepsilon})$ in Table 2 exhibits an improvement of ductility with decreasing and increasing T and $\dot{\varepsilon}$, respectively. Finally, the highest value and smallest scatter of ε_f is observed at $T = 300\,°C$ and $\dot{\varepsilon} = 0.001\,s^{-1}$, respectively.

4. Conclusions

Main results presented in this paper are as follows:

1. the steady state is not observed within the experimental stress-strain curves,

2. a decrease of ductility, as a property related to workability, is observed with an increase and a decrease of $\dot{\varepsilon}$ and T, respectively,

3. optimal values of $\dot{\varepsilon} = 0.001\,s^{-1}$, $T = 300\,°C$ with regard to the ductility are thus obtained.

Acknowledgements

References

[1] BARDI, F.—EVANGELISTA, E.—SPIGARELLI, S.—VUKCEVIC, M.: In.: 7th European Conference on Advanced Materials and Processes, EUROMAT 2001. Milano, AIM and FEMS 2001 (CD-ROM).

[2] HOU, J. P.—RUIZ, C.—TROJANOWSKI, A.: Mater. Sci. and Eng., *A283*, 2000, p. 181.

[3] SPIGARELLI, S.—CABIBBO, M.—EVANGELISTA, E.—BIDULSKÁ, J.: J. of Mat. Science, *38*, 2003, p. 81.

[4] PETERČÁKOVÁ, A.—POKORNÝ, I.: Kovove Mater., *41*, 2003, p. 389.

[5] McQUEEN, H. J.: Mater. Sci. and Eng., *A238*, 1998, p. 219.

[6] McQUEEN, H. J.—RYAN, N. D.: Mater. Sci. and Eng., *A322*, 2002, p. 43.

[7] McQUEEN, H. J.—KASSNER, M. E.: Scripta Mat., *51*, 2004, p. 461.

[8] BLAZ, L.—EVANGELISTA, E.: Mater. Sci. and Eng., *A207*, 1996, p. 195.

[9] McQUEEN, H. J.—AVRAMOVIC-CINGARA, G.—SAKARIS, P.: In.: Hot Workability of Steels and Light Alloys – Composites. Eds.: McQueen, H. J., Konopleva, E. V., Ryan, N. D. Montreal, The Metall. Society of the Canadian Inst. of Mining, Metall and Petroleum 1996, p. 69.

[10] RYUM, N.: Acta Mater., *17*, 1969, p. 269.

[11] NES, E.: Acta Mater., *20*, 1972, p. 499.

Table 2. Relationship between the fracture strain ε_f, the peak stress σ_p, the temperature T and the strain rate $\dot{\varepsilon}$

Strain rate (s^{-1})	Temperature $(°C)$	Peak stress (MPa)	Fracture strain $(-)$
0.001	300	65.951	2.8
	350	47.806	2.6
	400	35.822	2
	450	26.671	1.9
	500	15.963	1.5
0.01	300	71.539	4.7
	350	57.311	3.3
	400	43.778	2.3
	450	32.807	2.15
	500	21.299	1.65
0.1	300	85.963	6.3
	350	69.445	4.2
	400	54.815	3.265
	450	41.231	3
	500	29.237	0.952
1	300	112.543	6.268
	350	82.97	5.882
	400	66.883	5.457
	450	54.57	4.6
	500	44.48	2
5	300	127.056	3.953
	350	91.712	4
	400	80.551	4.42
	450	67.394	4.3
	500	41.882	0.456

[12] CABIBBO, M.—EVANGELISTA, E.—SPIGAREL-LI, S.: Mater. Sci. Forum, *396–402*, 2002, p. 807.

[13] CABIBBO, M.—EVANGELISTA, E.—SPIGAREL-LI, S.: Met. and Mater. Trans., *35A*, 2004, p. 293.

[14] VERLINDEN, B.—WOUTERS, P.—McQUEEN, H. J.—AERNOUDT, E.—DELAEY, L.—CAUWEN-BERG, S.: Mater. Sci. and Eng., *A123*, 1990, p. 229.

[15] EVANGELISTA, E..: In.: Hot Deformation of Aluminum Alloys. Eds.: Langdon T. G., Merchant H. D., Morris J. G., Zaidi M. A. The Minerals, Metals & Materials Society 1991, p. 121.

[16] McQUEEN, H. J.: In: Hot Deformation of Aluminum Alloys II. Eds.: Bieler, T. R., Lalli, L. A., MacEwen, S. R. Rosemont, Illinois, TMS Fall Meeting, The Minerals, Metals & Materials Society 1998, p. 31.

[17] McQUEEN, H. J.: Mater. Sci. and Eng., *A101*, 1988, p. 149.

[18] SAKAI, T.—JONAS, J. J.: Acta Mater., *32*, 1984, p. 189.

[19] WOUTERS, P.—VERLINDEN, B.—McQUEEN, H. J.—AERNOUDT, E.—DELAEY, L.—CAUWEN-BERG, S.: Mater. Sci. and Eng., *A123*, 1990, p. 239.

[20] EVANGELISTA, E.—GABRIELLI, F.—MENGUC-CI, P.—QUADRINI, E.—ANIONI, G.: In.: Innovation for Quality. Milan, Italy, AIM 1988, p. 205.

[21] OLAFFSON, P.—SANDSTROM, R.: Mat. Sci. Tech., *17*, 2001, p. 655.

[22] ESPEDAL, A.—GJESTLAND, H.—RYUM, N.—McQUEEN, H. J.: Scand. J. Metall., *18*, 1989, p. 131.